

## Characterization Studies, Photophysical and Aggregation Emission Properties of New Fluorescent 5-(4-(1*H*-phenanthro[9,10-*d*]imidazole-2-yl)phenyl)-2,4-dichlorophenyl-1,3,4-thiadiazole-2-amine

Merve Zurnaci<sup>1\*</sup>, Izzet Şener<sup>2</sup>, Mahmut Gür<sup>3</sup> and Nesrin Şener<sup>4</sup>

<sup>1</sup> Kastamonu University, Central Research Laboratory Application and Research Center, Kastamonu, Türkiye (ORCID: [0000-0002-2928-3492](https://orcid.org/0000-0002-2928-3492)), [mzurnaci@kastamonu.edu.tr](mailto:mzurnaci@kastamonu.edu.tr)

<sup>2</sup> Kastamonu Üniversitesi · Department of Food Engineering, Kastamonu, Türkiye (ORCID: 0000-0003-0540-7523), [isener@kastamonu.edu.tr](mailto:isener@kastamonu.edu.tr)

<sup>3</sup> Kastamonu University, Department of Chemistry, Kastamonu, Türkiye (ORCID: 0000-0001-9942-6324), [mahmutgur@kastamonu.edu.tr](mailto:mahmutgur@kastamonu.edu.tr)

<sup>4</sup> Kastamonu University, Department of Chemistry,, Kastamonu, Türkiye (ORCID: 0000-0001-5370-6048), [nsener@kastamonu.edu.tr](mailto:nsener@kastamonu.edu.tr)

(Received date: 24.04.2023 and Accepted date: 10.07.2023)

(DOI: [10.29228/JCHAR.69632](https://doi.org/10.29228/JCHAR.69632))

### Corresponding Author :

**CITE :** M. Zurnaci, I. Şener, M. Gür and N. Şener, “Characterization Studies, Photophysical and Aggregation Emission Properties of New Fluorescent 5-(4-(1*H*-phenanthro[9,10-*d*]imidazole-2-yl)phenyl)-2,4-dichlorophenyl-1,3,4-thiadiazole-2-amine” *J Characterization*, vol. 3, no. 2, pp 47-59, July, 2023, doi:10.29228/JCHAR.69632

### Abstract

Thanks to their chemical, thermal, photophysical, and photochemical properties, phenanthroimidazole derivative compounds attract attention in optoelectronic device technology, especially in OLEDs. For this reason, phenanthroimidazole derivatives are the most promising compounds for these applications in the future. In this study, the -diCl bearing phenanthroimidazole compound was synthesized, characterized, and investigated in detail the photophysical and aggregation properties. Spectroscopic studies for its characterization used <sup>1</sup>H-NMR, ATR-IR, and detailed LCMS-MS (mass and product ion scan). The absorption and emission spectra of *diCl-PHN* have been recorded with solvents of different polarities at room temperature. *diCl-PHN* exhibit high fluorescence quantum yield in DMSO with 0.78. CIE chromaticity diagram results of *diCl-PHN* were obtained and displayed good intensity. Additionally, aggregation properties were recorded at seven different water concentrations (water/DMSO %). With the results obtained from the study, it was concluded that this phenanthroimidazole derivative compound is a suitable molecule for fluorescent applications.

**Keywords:** *diCl* bearing phenanthroimidazole, blue fluorescence, quantum yield, solvent effect-chromaticity, aggregation effects.

## Yeni Floresan 5-(4-(1*H*-fenantro[9,10-*d*]imidazol- 2-il)fenil)-2,4-diklorofenil-1,3,4-tiyadiazol-2-amin'in Karakterizasyon Çalışmaları, Fotofiziksel ve Agregasyon Emisyon Özellikleri

### Öz

Fenantroimidazol türevi bileşikler kimyasal, termal, fotofiziksel ve fotokimyasal özellikleri sayesinde optoelektronik cihaz teknolojisinde özellikle OLED'lerde dikkat çekmektedir. Bu nedenle fenantroimidazol türevleri, gelecekte bu uygulamalar için en umut verici bileşiklerdir. Bu çalışmada -*diCl* içeren fenantroimidazol

bileşigi sentezlenmiş, karakterize edilmiş, fotofiziksel ve agregasyon özellikleri detaylı olarak incelenmiştir. Karakterizasyonu için spektroskopik çalışmalarda <sup>1</sup>H-NMR, ATR-IR ve ayrıntılı LCMS-MS (kütle ve ürün iyon taraması) kullanılmıştır. *diCl-PHN*'nin absorpsiyon ve emisyon spektrumları, oda sıcaklığında farklı polaritelere sahip çözücüler ile kaydedilmiştir. *diCl-PHN*, 0.78 ile DMSO'da yüksek floresans kuantum verimi sergiledi. *diCl-PHN*'nin CIE kromatiklik diyagramı sonuçları elde edildi ve iyi yoğunluk gösterdi. Ek olarak, yedi farklı konsantrasyonunda (su/DMSO %) agregasyon özellikleri kaydedildi. Çalışma sonucunda elde edilen sonuçlarla bu fenantroimidazol türevi bileşiğin çeşitli floresan uygulamaları için uygun bir molekül olduğu sonucuna varılmıştır.

**Anahtar Kelimeler:** *diCl* İçeren Fenantroimidazol, Mavi Floresans, Kuantum Verimi, Solvent Etkisi-Kromatiklik, Agregasyon Etkileri.

## 1. Introduction

In recent years, research on fluorescent organic compounds; has grown exponentially due to their importance in technological applications [1], [2]. Heterocyclic compounds with  $\pi$ -conjugated systems have played an essential role due to their broad applications among fluorescence organic compounds [3], [4]. Nowadays, different matrices, additives, and production methods of heterocyclic compounds have been the research subject for many different studies [5]–[8]. These compounds are one of the most studied molecules in optical sensor technology, thanks to their excellent spectral (absorption, emission, etc.) and analyte detection properties [9]. Among the heterocyclic compounds, phenanthroimidazole derivatives are remarkable fluorescent compounds phenanthrene and imidazole containing, which are widely used optoelectronic [10], [11], electrochemical cell [12], sensors [13], diodes [14]. Phenanthroimidazoles are excellent materials used as emission emitters in organic light-emitting diodes (OLEDs) because they have electron transport and hole-blocking properties [10], [15]–[18]. 1,3,4-thiadiazoles are considerable compounds frequently encountered in medicinal [19], [20] and pharmaceutical chemistry, polymer or monomer and current material technology [20]–[22]. There are several reports on the synthesis, characterization, surface-morphological, electrical, and optical properties of phenanthroimidazole-1,3,4-thiadiazole hybrid compounds [14], [23], [24]. In most of these reports, it was emphasized that these compounds have strong fluorescence properties. The choice of donor, recipient, or other units plays a vital role in obtaining an ideal dark blue emissive compound [25]. Therefore, the design of new donor-acceptor (D-A) molecules is the fundamental step for organic fluorescent compounds [25], [26]. The phenanthroimidazole unit will contribute to the photophysical properties by increasing the fluorescence efficiency due to the  $\pi$  electron system in its structure, having good electron-withdrawing ability and strong photophysical properties [29]. Due to the mentioned advantages, it was decided to choose the hybrid structure in the synthesis of the compounds.

This paper, new fluorescent *-diCl* substituted compound was synthesized so as to determines its fluorescence characterization. Regarding the fluorescent characterization of the new compound, it covers four basic processes: (i) absorption and emission properties; (ii) quantum yield (q<sub>f</sub>); (iii) fluorescence properties in solvents of different polarity; (iv) Aggregation Emission studies. Considering the growing interests in fluorescent organic compounds, this work presents a detail studies of the fluorescent characterization of new compound based on phenanthroimidazole-1,3,4-thiadiazole hybrid compound.

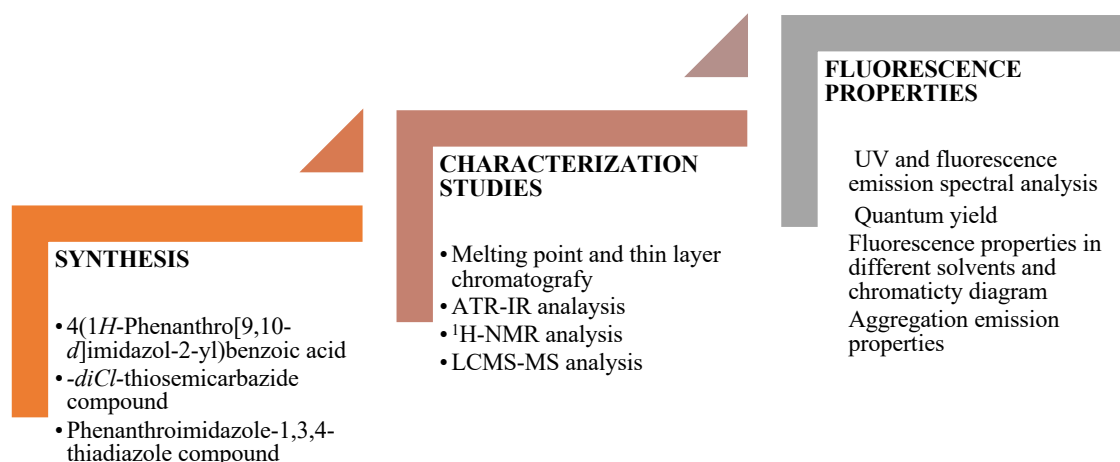


Fig. 1. Scope of the study

## 2. Materials and Method

### 2.1. Chemicals and instrumentations

Solvents and chemicals used in the synthesis stages are for analysis and are of analytical grade (Merck and Sigma Aldrich). The solvents used in the measurements were spectroscopic grade. Thin layer chromatography and melting point (Stuart SMP30) were used in the preliminary analysis for characterization. <sup>1</sup>H-NMR measurements were carried out by Bruker Ultrashield 300 MHz NMR spectrometer. UV-Vis (Shimadzu UV Pharmaspec) and fluorescence (Horiba Fluoromax-4) spectrophotometers investigated the absorption and emission properties. ATR-IR analyses were performed using Bruker Alpha. Mass and product ion scanning studies were recorded using the Shimadzu brand LCMS-MS/8030 Plus model (LCMS-MS).

#### 2.1.1. Synthesis of 5-(4-(1*H*-phenanthro[9,10-*d*]imidazole-2-yl)phenyl)-2,4-dichlorophenyl-1,3,4-thiadiazole-2-amine diCl-PHN

4-(1*H*-phenanthro[9,10-*d*]imidazole-2-yl)benzoic acid was obtained by the condensation reaction between aldehyde and phenanthrenequinone [13]. The reaction was carried out using ammonium acetate and glacial acetic acid (%99.9). As a result, 4-(1*H*-phenanthro[9,10-*d*]imidazole-2-yl)benzoic acid was obtained, with yields of 91%. This method will synthesize phenanthro[9,10-*d*]imidazole compound in high yield without any catalyst. 2,4-dichloro phenyl thiosemicarbazide was synthesized as described in the literature [30].

In the last part of the synthesis steps, the reaction of 4-(1*H*-Phenanthro[9,10-*d*]imidazole-2-yl)benzoic acid compound and 2,4-dichloro thiosemicarbazide was carried out. Thus, the synthesis of a 1,3,4-thiadiazole derivative containing phenanthroimidazole structure was carried out. 4-(1*H*-phenanthro[9,10-*d*]imidazole-2-yl)benzoic acid (0.5 g, 1.5 mmol), 2,4-dichloro phenyl thiosemicarbazide (0.325 g, 1.5 mmol) and POCl<sub>3</sub> (0.42 mL, 4.5 mmol) were added into 100 mL round-bottomed flask. Reaction conditions: 4-5 hours and 90 °C. The resulting mixture was precipitated with ice water. The mixture was adjusted with ammonia (%20) to pH = 7-8 the next day. This compound was obtained as a brown solid, dried, and purified in DMSO. Yield: (89%), melting point (mp): 310 °C; ATR-IR (cm<sup>-1</sup>) v: 3148.99 cm<sup>-1</sup> (stretching, -NH), 3058.78; 2987,63; 2907.31 cm<sup>-1</sup> (Aromatic, C-H), 1680.73 cm<sup>-1</sup> (bending, -NH); 1606.46 cm<sup>-1</sup> and 1528.40 cm<sup>-1</sup> (-C=N-), 1465.87-14 cm<sup>-1</sup> (-C=C-), 1093.83 cm<sup>-1</sup> (stretching, C-Cl), 708.97 cm<sup>-1</sup> (-C-S-C-). <sup>1</sup>H-NMR (ppm): 9.00-8.80 (4H, d, aromatic in benzene ring), 8.65 (t, 2H), 8.45 (t, 2H), 8.18-8.10 (t, 2H), 7.76 (q, 2H), 7.66 (q, 2H), 8.21 (s, 1H, -NH), 7.53 (s, 1H) detailed in Fig. 4. LCMS-MS (ESI-*m/z*) (M+H)<sup>+</sup>: Calculated/found: 538.45/538.00. The route of synthesis is given in Fig 2.

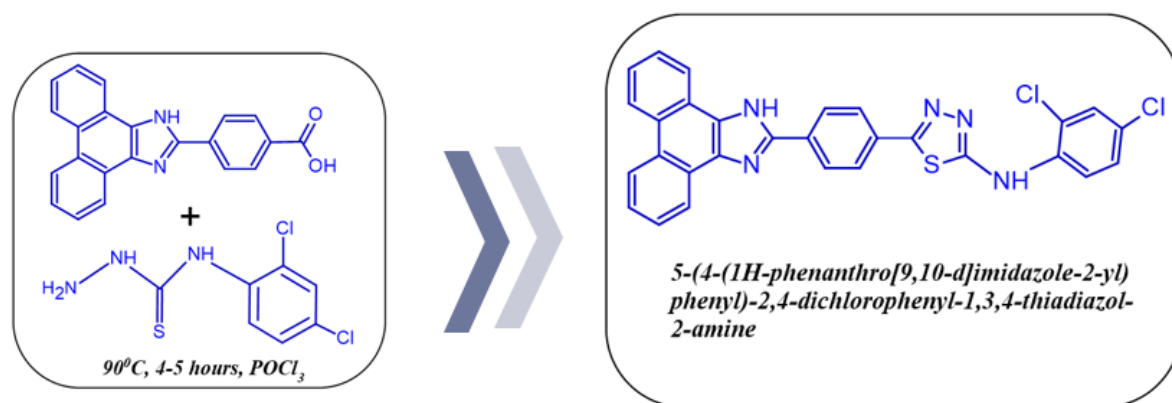

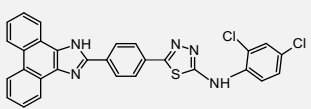


Figure 2. Synthesis of diCl-PHN

Table 1. Experimental data of diCl-PHN

Compound	Molecular structure	Molecular formula	Molecular weight	Reaction yield (%)	Product Colour	Melting point
		C <sub>29</sub> H <sub>17</sub> Cl <sub>2</sub> N <sub>5</sub> S	538,45	%89	Brown	310 °C

### 3. Results and Discussion

#### 3.1. Characterization Studies

The scheme of synthesis for the compound is summarized in **Fig. 2**. The structure of the new 1,3,4-thiadiazole compound containing *-diCl* substituted phenanthroimidazole was confirmed by extensive spectroscopic studies. The ATR-IR transmittance-wavelength values of the synthesized compound are given in **Fig. 3**.

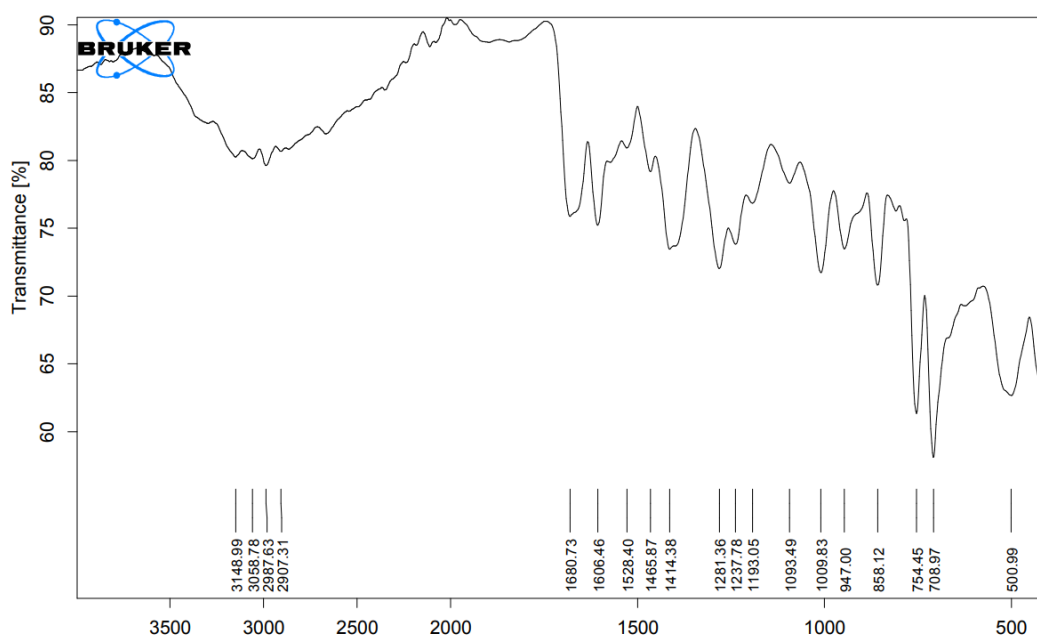


Figure 3. ATR-IR spectra of diCl-PHN

**In the ATR-IR spectrum** of diCl-PHN, peaks of the carbonyl group and hydroxyl group vibrations in the starting reagent were not observed. Instead of these peaks, in the ATR-IR spectrum of the synthesized compound, vibrations of groups such as  $-NH$ ,  $C=N$ ,  $C-S-C$ , and different peaks appeared according to different substitution groups. IR signals resulting from  $-NH$  stretching are seen at  $3148.99\text{ cm}^{-1}$ . Aromatic  $C-H$  stretching vibrations are observed at  $3058.78$ ,  $2987.63$ , and  $2907.31\text{ cm}^{-1}$ . It was determined to belong to the peak  $-NH$  bending vibration seen at  $1680.73\text{ cm}^{-1}$ . Other  $\nu_{max}$  values are observed  $1465.87\text{ cm}^{-1}$  stretching vibrations  $-C=C-$ ,  $1606.46\text{ cm}^{-1}$  and  $1528.40\text{ cm}^{-1}$   $C=N$  stretching vibrations on the 1,3,4-thiadiazole structure,  $1093.83\text{ cm}^{-1}$  stretching  $-C-Cl$ ,  $708.97\text{ cm}^{-1}$  stretching vibrations  $C-S-C$ .

**Nuclear magnetic resonance ( $^1H$ -NMR)** spectra were measured in DMSO-*d*<sub>6</sub>. When the  $^1H$ -NMR spectrum of diCl-PHN seen in Figure 4 is examined, H19, H20, H21, and H22 protons were observed between 9.00-8.80 ppm as two doublet peaks in the benzene ring; triplet peak at 8.65 ppm protons H6 and H11; triplet peak at 8.45 ppm protons H1 and H13; the triplet peak at 8.18-8.10 ppm were H32 and H34 protons; the quartet peak at 7.76 ppm were H5 and H12 protons; the quartet peak at 7.66 ppm H3 and H14 protons. The proton H29 in  $-NH$  was determined as the singlet peak at 8.21 ppm. The proton H33 between Cl atoms in benzene was determined as the singlet peak at 7.53 ppm. In the  $^1H$ -NMR spectra of all the compounds, 16 aromatic protons were detected at the

9.00–7.49 ppm range. All these results confirmed the successful synthesis of *diCl-PHN*. The  $^1\text{H-NMR}$  dates are given in **Table 2**.

Table 2.  $^1\text{H-NMR}$  data ( $\delta$ , ppm, in  $\text{DMSO-}d_6$ )

Compound	$\delta$ , ppm and J values
<i>diCl-PHN</i>	8.88 (d, J = 2.8 Hz, 2H), 8.86 (d, 2.9 Hz, 2H), 8.65 (t, J = 7.9 Hz, 2H), 8.45 (t, J = 7.7 Hz, 2H), 8.21 (s, 1H, -NH), 8.18 – 8.10 (m, 2H), 7.76 (q, J = 9.9, 5.0 Hz, 2H), 7.66 (q, J = 7.0, 3.4 Hz, 2H), 7.53 (s, 1H)

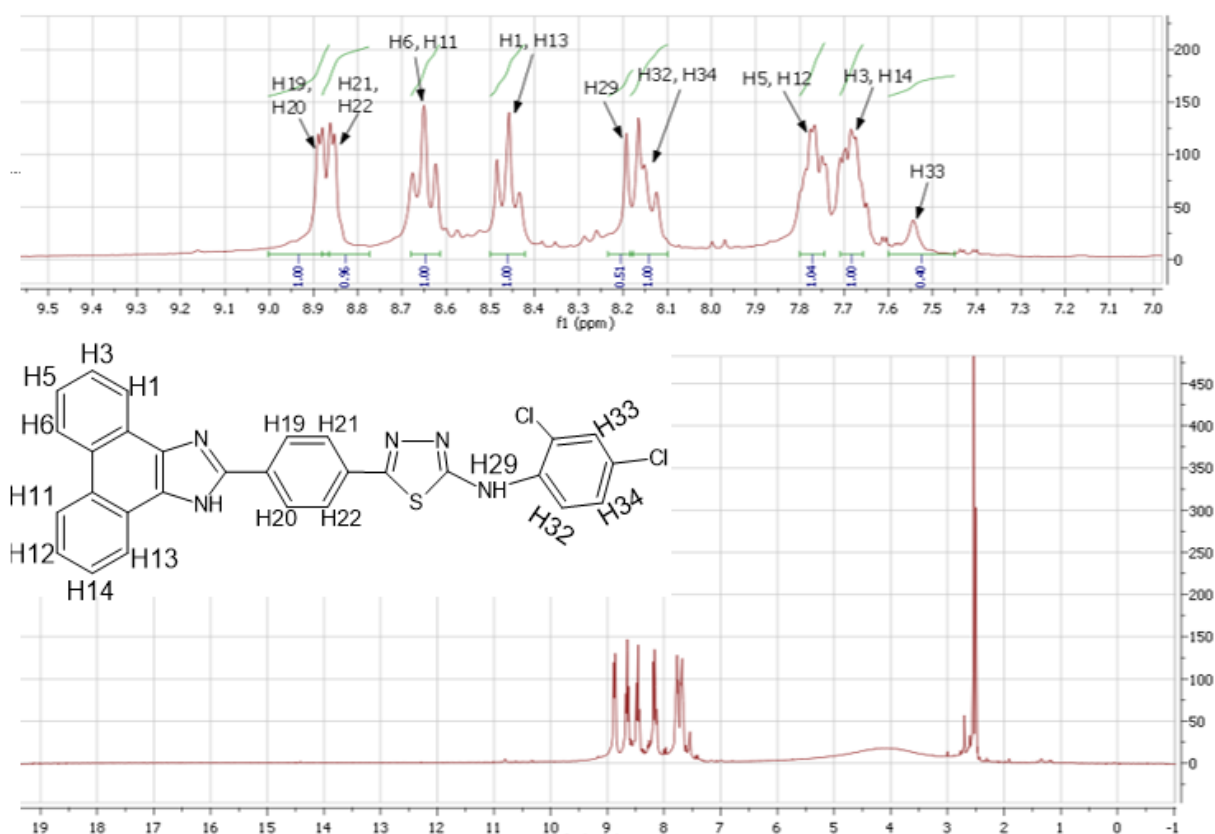


Figure 4.  $^1\text{H-NMR}$  spectra of *diCl-PHN*

**Mass analysis of *diCl-PHN*;** In this spectroscopic method, the molecular weight of *diCl-PHN* and the molecular weights obtained due to fragmentation will be revealed. LCMS/MS studies were conducted using a Shimadzu-LCMS-8030 Plus Mass spectrometer with an electrospray ionization source. This analysis was performed by infusion of aqueous *diCl-PHN* solution and dissolved in DMSO. Both positive and negative ion electrospray mass spectra were recorded. Conditions: Mobile Phase A (1/1000 (formic acid/dH<sub>2</sub>O)), Mobile Phase B (1/1000 (formic acid/ethanol)), pump B (70%), analysis time (1 min.), DL temperature (250 oC), total flow (0.3 mL/min), injection volume (0.1  $\mu\text{L}$ ), scan type (Q3). A precursor ion scan of 500–540 and a product ion scan were studied at an  $m/z$  200–500 range.

The mass spectrum obtained for *diCl-PHN* is given in **Fig. 5** as a positive scan. As expected, *diCl-PHN* showed Calculated: 538.45; LC-MS/MS: 538.00  $[\text{M}+\text{H}]^+$ . The predicted fragmentation mode of *diCl-PHN* is presented. The precursor ion (I) fragmentations were determined by product ion scan in positive ion. MS/MS peaks (II, III, IV, and V) were given in **Supplementary File (S-Fig. 1)**. The main base fragmentation ion peak ( $m/z$  293.75) came from the structure of 2-phenyl-1*H*-phenanthro-[9,10-*d*]imidazole. The other fragmentation ion ( $m/z$  319.15) came from the cleavage of in 1,3,4-thiadiazole structure NH-NH bond. In addition, the fragmentation ion gave at  $m/z$  391.00 by the cleavage of substituted 2,4-*diCl*-phenyl structure in *diCl-PHN*. When the findings obtained as a result of mass analysis and other spectroscopic methods were evaluated, the molecular structure of the synthesized *diCl-PHN* was clarified, and its accuracy was proven.

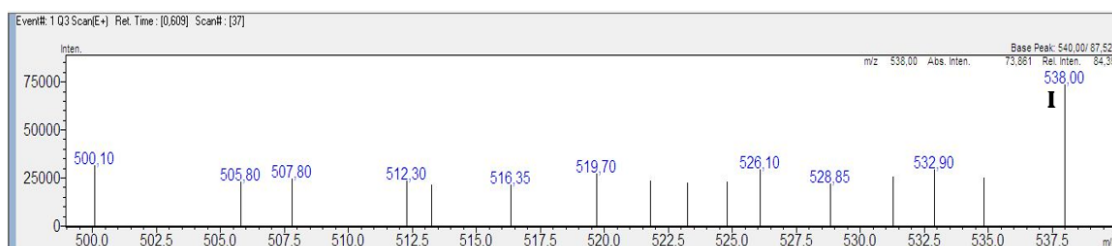


Figure 5. LCMS-MS spectrum of the *diCl-PHN* (Calculated: 538.45, LC-MSMS: 538.00  $[M+H]^+$ )

### 3.2. Fluorescence Characterization

- Investigation of fluorescence characterization of *diCl-PHN*;
- Determination of absorption and emission properties with UV-visible and fluorescence spectrophotometers
- Stokes' shift
- Molar absorption coefficient
- Singlet energy level
- Quantum yield (qf)
- Investigation of fluorescence properties in solvents of different polarity
- It covers Aggregation Emission studies

The fluorescence characterization of *diCl-PHN* was determined using ultraviolet–visible (UV–vis) and fluorescence spectrometers. The absorption spectra were measured in the 300–700 nm range and studied in DMSO at room temperature. Steady-state fluorescence emission spectra were measured by a fluorescence spectrophotometer (Horiba Fluoromax-4). The excitation and emission slit interval was 1 nm, and the integration (measurement) time was 0.1 s. The concentration of *diCl-PHN* was  $10^{-5}$  M in the DMSO solution, and measurements were taken at room temperature. Maximum absorption and emission wavelengths, Stokes' shift, molar extinction coefficient, and quantum yield of *diCl-PHN* are presented in Table 2. Also, the aggregation-induced emission behaviours of the *diCl-PHN* were investigated in detail.

The maximum absorption wavelength of the *diCl-PHN* in DMSO was 373 nm, the maximum emission wavelength was 435 nm, and the Stokes' shift value was 62 (Figure 6). The color change of *diCl-PHN* in DMSO under daylight and UV lamp (365 nm) is shown in Picture 1. It has been observed that *diCl-PHN*, which is transparent in daylight, emits blue under UV light. As can be seen from the absorption and emission spectra, *diCl-PHN* shows blue emission in solution (DMSO) at a steady state.

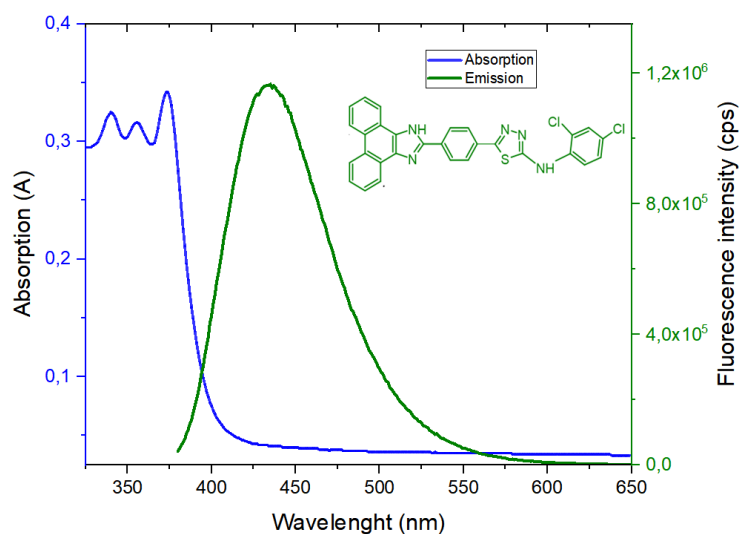


Figure 6. Absorption and emission spectra of *diCl-PHN* in DMSO ( $10^{-5}$  M)



Picture 1. The color of *diCl-PHN* in daylight (left) and UV lamp (right) in DMSO

The quantum yield is one of the essential properties of a fluorescent compound [31], [32]. It is usually made sense by the relationship between the number of photons absorbed and the number of photons emitted [32], [33]. Compounds with high quantum yields, such as rhodamines and fluorescein, display bright and strong emissions [34], [35]. The quantum yield is best expression by a Jablonski diagram [36], [37]. In this study, the fluorescence quantum yield of *diCl-PHN* is calculated with the help of **Equation 1**. As shown in **Table 3**, the quantum yield of *diCl-PHN* was 0.78 in the DMSO.

$$\Phi_{\bar{o}} = \frac{A_s I_{\bar{o}} (n_{\bar{o}})^2}{A_{\bar{o}} I_s (n_s)^2} \Phi_s \quad \Phi_s = 0.94 \text{ (Perylene in cyclohexane)} \quad [\text{Eq. 1}]$$

The molar absorption coefficient ( $\epsilon$ ) was calculated in **Equation 2** using the Beer-Lambert law and a standard 1 cm in the tub. The singlet energy level ( $E_s$ ) of *diCl-PHN* was calculated in **Equation 3**. The molar absorption coefficient of *diCl-PHN* was 34200 (L/mol.cm), and the singlet energy level was 76.99 (kcal/mol).

$$A = \epsilon cl \quad [\text{Eq. 2}] \quad E_s = \frac{hc}{\lambda} \quad [\text{Eq. 3}]$$

Table 3. Fluorescence properties data for *diCl-PHN* ( $\lambda_{\text{max}}$ , Stokes' shift, molar excitation efficient, singlet energy level and quantum yield)

Compound	Absorbance ( $\lambda_{\text{max}}$ )	Emission ( $\lambda_{\text{max}}$ )	Stokes' Shift ( $\lambda$ )	Molar Excitation Coefficient (L mol <sup>-1</sup> cm <sup>-1</sup> )	Es (Singlet Energy Level)	Quantum Yield (Q <sub>f</sub> )
<i>diCl-PHN</i>	373	435	62	34200	76.99	0.78

### 3.2.1. Solvent effect on fluorescence properties and chromaticity diagram

Solvent polarity has an important place in organic molecules' optical and photophysical properties [38]. In this section, we have investigated the effects of solvent polarity on the absorption and fluorescence spectra of *diCl-PHN*. The absorption and emission spectrum of *diCl-PHN* in solvents with different polarities were measured. In this context, Dichloromethane, Chloroform, Acetonitrile, Dimethylformamide and Dimethylsulfoxide were used. The change in fluorescence characteristics according to the polarity constants was investigated in detail (low polar to high polar).

*diCl-PHN* excited at 370, 371, 369, 371, and 373 nm display fluorescence in the blue emission region in all solutions. **Fig. 7** shows the absorption (a), fluorescence emission (b), and chromaticity diagrams for all solutions. Maximum absorbance and fluorescence emission wavelengths depending on the polarity constants of the compound are given in **Fig. 7 (c)**. When **Fig. 7 a, b, and c** are examined, it is seen that the maximum absorption points are similar. It was determined that the lowest fluorescence emission wavelength and Stokes shift was DMF and the highest was DCM. With the increasing polarity of solvents, absorption is relatively similar; the emission peak is redshifted (excluding DMSO). The spectral shifts of *diCl-PHN* resulting from the excited and ground state dipole moment appear to occur in absorption and emission.

The color of *diCl-PHN* in DMSO was changed from blue to green concerning the polarity of the solvent. The color and emission region of fluorescent compounds can be determined using the Commission Internationale de l'Eclairage (CIE) chromaticity diagram. The changes in the CIE coordinates show the changes in the spectral region and compare the  $\lambda_{\text{max}}$  of different polarity solvents. In literature, blue emitters generally show emissions of 0.15, 0.10 (x;y) (CIE). The coordinates obtained in different polarity solvents are given in **Table 3**. These coordinates are situated in the blue region (**Fig. 7 d**), and this result indicates a potential compound as a blue light emitter in optoelectronic technologies.

Table 3. Absorption, emission and CIE 1931 coordinates in different polarity

Solvents	Abs. (max nm)	Emis.(max nm)	CIE coordinates (x,y)
DCM	370	447	(0.150, 0.117)
CHCl <sub>3</sub>	371	444	(0.151, 0.123)
ACN	369	437	(0.152, 0.093)
DMF	371	426	(0.154, 0.069)
DMSO	373	435	(0.152, 0.079)

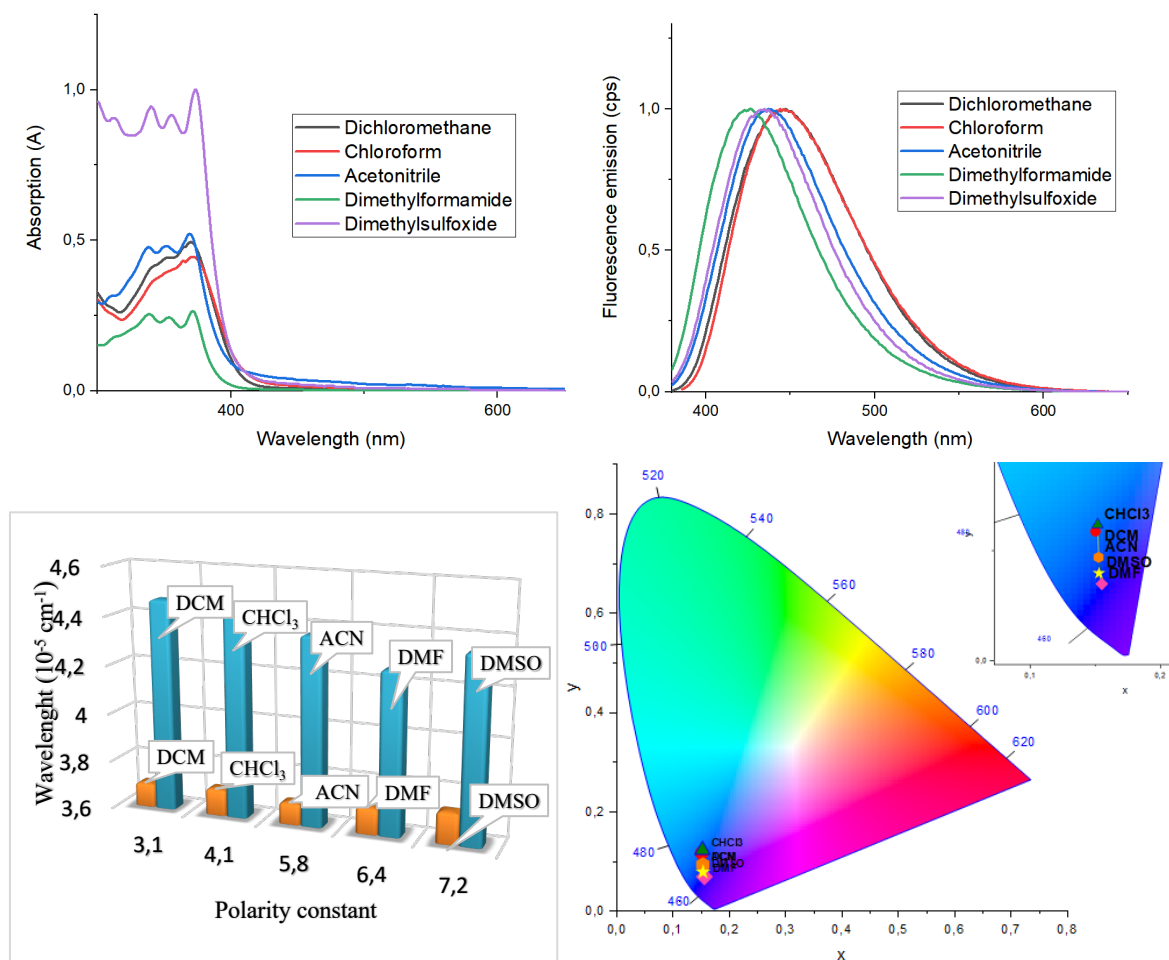


Figure 7. a) Absorption of diCl-PHN in solvents of different polarity b) Normalized fluorescence emission of diCl-PHN in solvents of different polarity c) Maximum absorption and emission points in solvents of different polarity d) diCl-PHN corresponding to the CIE 1931 XYZ color space changes in solvents of different polarity

### 3.2.2. Aggregation emission properties

When the structures of optoelectronic devices such as OLED are examined, one of the important parameters is "Aggregation Induced Emission" (AIE) [39]. Generally, fluorescent organic molecules emit bright light in dilute solutions, but their appearance changes as the concentration changes [40]. Aggregation is an undesirable factor for many applications where the light emitted by the molecule under the UV lamp becomes dimmer as the concentration increases [41], [42]. If the molecule is AIE, undesirable situations may be encountered during the device construction phases. Recently, aggregation studies of fluorescent organic molecules used in optoelectronic technology have been carried out [43], [44]. Fluorescence organic molecules, the tendency to aggregate, emission density, and change in quantum yield are examined [45]. The change in the percentage of water in the solution form of the molecule can cause a hydrophobic effect on the molecules, and restriction of intramolecular rotation

and aggregation can occur. Because with the increasing amount of water, hydrophobic structures are stacked together [46].

AIE measurements of the *diCl-PHN* in solution were made by varying the DMSO-water ratios (values between 0-90%). *diCl-PHN* was excited at a wavelength of 373 nm, and fluorescence measurements were performed (Figure 8). The change in fluorescence intensity, which varies according to the DMSO-water ratios, was examined. In Fig. 8, a decrease in the emission intensity is observed as the amount of water in the solution increases.

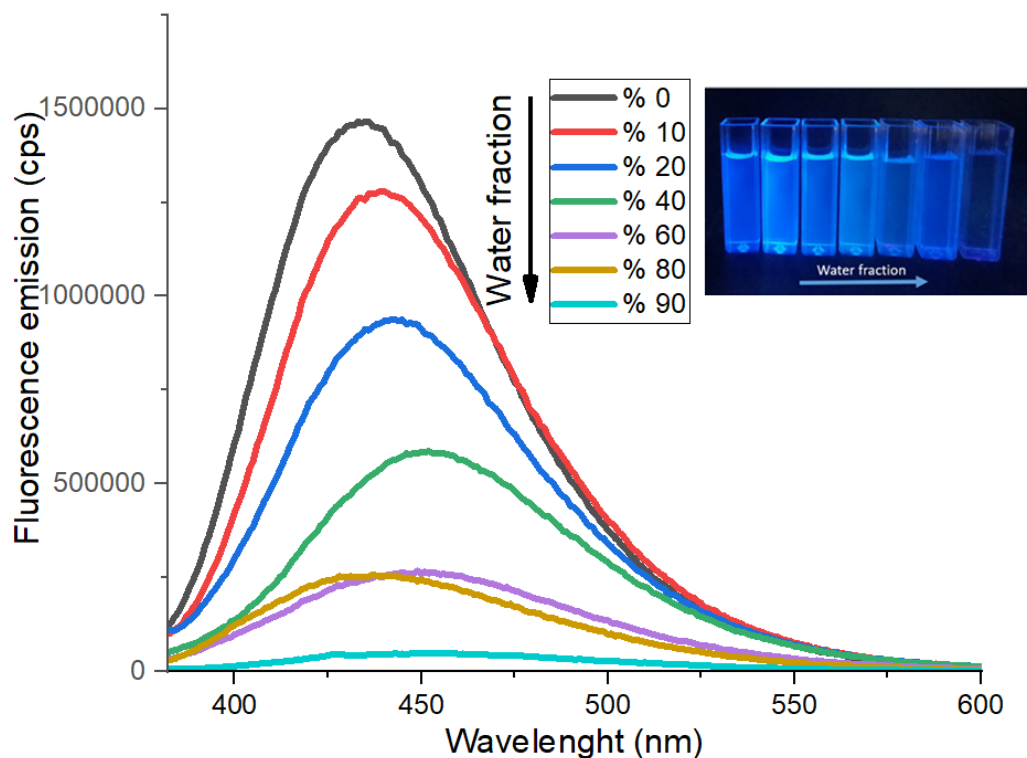


Figure 8. Fluorescence emission spectrum and images under UV lamp due to different water fractions (%0-90).

#### 4. Conclusions

We have represented phenanthroimidazole compounds derivatized with different substituents and positions in our previous studies. In this study, we synthesized fluorescent *-diCl* substituted phenanthroimidazole monomer. All spectroscopic results confirmed the successful synthesis of *diCl-PHN*. In conclusion, this paper highlighted the spectroscopic studies and fluorescence characterization of the new phenanthroimidazole compound in detail. *diCl-PHN* excited at the maximum absorption point presented good fluorescence between 426-447 nm. *diCl-PHN* presented a high quantum yield (0.78) in DMSO. The fluorescence parameters (absorption, emission, and CIE coordinates) were characterized in five different polarity solvents. Accordingly, the chromaticity diagram and coordinates were recorded. For *diCl-PHN*, AIE measurements were carried out in Water /DMSO (%0-90). A decrease in the emission intensity and brightness under the UV lamp was recorded as the amount of water in the solution increased. In this case, all photophysical measurements indicated that *diCl-PHN* has the good quantum yield and fluorescence properties, making it a potential application in materials chemistry, especially optic materials.

#### 5. Acknowledge

We thank the Central Research Laboratories of Kastamonu University for contributing to our laboratory work.

#### Declaration of Ethical Standards

The author(s) of this article declare that the materials and methods used in their studies do not require ethical committee approval and/or legal-specific permission.

### Authors' Contributions

**M. Z.:** Synthesis, Spectroscopic studies, Photophysical and Aggregation measurements, Writing—original draft.

**İ. Ş.:** Methodology, Equipment supply, Editing & Read.

**M. G.:** Methodology, Equipment supply, Editing & Read.

**N. Ş.:** Equipment supply, Editing & Read.

### Conflict of Interest

There is no conflict of interest in this study.

### References

- [1] Y. Yang *et al.*, “Fluorescent Organic Small Molecule Probes for Bioimaging and Detection Applications,” *Molecules*, vol. 27, no. 23, p. 8421, Dec. 2022, doi: 10.3390/molecules27238421.
- [2] G. Vargas-Nadal *et al.*, “Fluorescent Multifunctional Organic Nanoparticles for Drug Delivery and Bioimaging: A Tutorial Review,” *Pharmaceutics*, vol. 14, no. 11, p. 2498, Nov. 2022, doi: 10.3390/pharmaceutics14112498.
- [3] T. Wang, N. Zhang, W. Bai, and Y. Bao, “Fluorescent chemosensors based on conjugated polymers with N-heterocyclic moieties: two decades of progress,” *Polymer Chemistry*, vol. 11, no. 18, pp. 3095–3114, 2020, doi: 10.1039/D0PY00336K.
- [4] X. Zhao, S. T. Chaudhry, and J. Mei, “Heterocyclic Building Blocks for Organic Semiconductors,” 2017, pp. 133–171.
- [5] S. Das, R. Fröhlich, and A. Pramanik, “Synthesis and Fluorescent Properties of a New Class of Heterocycles of Isoindole Fused Imidazoles with Phenolic Subunits,” *Organic Letters*, vol. 8, no. 19, pp. 4263–4266, Sep. 2006, doi: 10.1021/ol061520n.
- [6] G. Brocks and A. Tol, “Electronic structure of heterocyclic ring chain polymers,” *Synthetic Metals*, vol. 101, no. 1, pp. 516–517, 1999, doi: 10.1016/S0379-6779(98)01416-7.
- [7] Y. Ooyama, T. Nakamura, and K. Yoshida, “Heterocyclic quinol-type fluorophores. Synthesis of novel imidazoanthraquinol derivatives and their photophysical properties in benzene and in the crystalline state,” *New Journal of Chemistry*, vol. 29, no. 3, pp. 447–456, 2005, doi: 10.1039/b410311d.
- [8] V. Ramkumar and P. Kannan, “Novel heterocyclic based blue and green emissive materials for optoelectronics,” *Optical Materials*, vol. 46, pp. 314–323, 2015, doi: 10.1016/j.optmat.2015.04.038.
- [9] V. Naresh and N. Lee, “A Review on Biosensors and Recent Development of Nanostructured Materials-Enabled Biosensors,” *Sensors*, vol. 21, no. 4, p. 1109, Feb. 2021, doi: 10.3390/s21041109.
- [10] M. Idris *et al.*, “Phenanthro[9,10- d ]triazole and imidazole derivatives: high triplet energy host materials for blue phosphorescent organic light emitting devices,” *Materials Horizons*, vol. 6, no. 6, pp. 1179–1186, 2019, doi: 10.1039/C9MH00195F.
- [11] Z. Huang *et al.*, “Highly efficient green organic light emitting diodes with phenanthroimidazole-based thermally activated delayed fluorescence emitters,” *Journal of Materials Chemistry C*, vol. 6, no. 9, pp. 2379–2386, 2018, doi: 10.1039/c7tc05576e.
- [12] B. N. Bideh, M. Moghadam, A. Sousaraei, and B. S. Arani, “Phenanthroimidazole as molecularly engineered switch for efficient and highly long - lived light - emitting electrochemical cell,” *Scientific*

- [13] S. M. Hwang, J. B. Chae, and C. Kim, “A Phenanthroimidazole-based Fluorescent Turn-Off Chemosensor for the Selective Detection of Cu<sup>2+</sup> in Aqueous Media,” *Bulletin of the Korean Chemical Society*, vol. 39, no. 8, pp. 925–930, 2018, doi: 10.1002/bkes.11526.
- [14] M. Zurnacı, F. Ünal, S. Demir, M. Gür, N. Şener, and İ. Şener, “Synthesis of a new 1,3,4-thiadiazole-substituted phenanthroimidazole derivative, its growth on glass/ITO as a thin film and analysis of some surface and optoelectronic properties,” *New Journal of Chemistry*, 2021, doi: 10.1039/D1NJ04375G.
- [15] Y. Yuan *et al.*, “Phenanthroimidazole-derivative semiconductors as functional layer in high performance OLEDs,” *New Journal of Chemistry*, vol. 35, no. 7, pp. 1534–1540, 2011, doi: 10.1039/c1nj20072k.
- [16] S. Kula *et al.*, “Phenanthro[9,10-d]imidazole with thiophene rings toward OLEDs application,” *Dyes and Pigments*, vol. 159, pp. 646–654, 2018, doi: 10.1016/j.dyepig.2018.07.014.
- [17] J. Tagare and S. Vaidyanathan, “Recent development of phenanthroimidazole-based fluorophores for blue organic light-emitting diodes (OLEDs): an overview,” *Journal of Materials Chemistry C*, vol. 6, no. 38, pp. 10138–10173, 2018, doi: 10.1039/C8TC03689F.
- [18] Y. Zhang *et al.*, “Synthesis and characterization of phenanthroimidazole derivatives for applications in organic electroluminescent devices,” *Journal of Materials Chemistry*, vol. 21, no. 22, pp. 8206–8214, 2011, doi: 10.1039/c1jm10326a.
- [19] G. Serban, O. Stanasel, E. Serban, and S. Bota, “2-Amino-1,3,4-thiadiazole as a potential scaffold for promising antimicrobial agents,” *Drug Design, Development and Therapy*, vol. Volume 12, pp. 1545–1566, May 2018, doi: 10.2147/DDDT.S155958.
- [20] D. Visagaperumal, J. Ramalingam, and V. Chandy, “Issue 01 Citation: Visagaperumal D, Ramalingam J, Chandy V (2018) 1, 3, 4-Thiadiazoles: An Overview,” *Curr Res Bioorg Org Chem*, vol. 2018, no. 01, p. 103, 2018, doi: 10.29011/CRBOC.
- [21] Y. Hu, C. Li, X. Wang, Y. Yang, and H. Zhu, “1,3,4-Thiadiazole: Synthesis, Reactions, and Applications in Medicinal, Agricultural, and Materials Chemistry,” *Chemical Reviews*, vol. 114, pp. 5572–5610, 2014, doi: 10.1021/cr400131u.
- [22] T. A. Salman *et al.*, “Effect of 1,3,4-Thiadiazole Scaffold on the Corrosion Inhibition of Mild Steel in Acidic Medium: An Experimental and Computational Study,” *Journal of Bio- and Tribo-Corrosion*, vol. 5, no. 2, pp. 1–11, 2019, doi: 10.1007/s40735-019-0243-7.
- [23] M. Zurnacı, İ. Şener, M. Gür, and N. Şener, “Study on Photophysical Properties of Novel Fluorescent Phenanthroimidazole-Thiadiazole Hybrid Derivatives,” *Journal of Fluorescence*, vol. 32, no. 3, pp. 1155–1169, May 2022, doi: 10.1007/s10895-022-02916-3.
- [24] Y.-X. Hu, G.-W. Zhao, Y. Dong, Y.-L. Lü, X. Li, and D.-Y. Zhang, “New rhenium(I) complex with thiadiazole-annulated 1,10-phenanthroline for highly efficient phosphorescent OLEDs,” *Dyes and Pigments*, vol. 137, pp. 569–575, Feb. 2017, doi: 10.1016/j.dyepig.2016.10.048.
- [25] Anupriya, K. R. J. Thomas, M. R. Nagar, Shahnawaz, and J.-H. Jou, “Phenanthroimidazole substituted imidazo[1,2-a]pyridine derivatives for deep-blue electroluminescence with CIE<sub>y</sub> ~ 0.08,” *Journal of Photochemistry and Photobiology A: Chemistry*, vol. 423, p. 113600, 2022, doi: <https://doi.org/10.1016/j.jphotochem.2021.113600>.
- [26] L. Duan, J. Qiao, Y. Sun, and Y. Qiu, “Strategies to Design Bipolar Small Molecules for OLEDs: Donor-Acceptor Structure and Non-Donor-Acceptor Structure,” *Advanced Materials*, vol. 23, no. 9, pp. 1137–1144, Mar. 2011, doi: 10.1002/adma.201003816.
- [27] Z. Wang *et al.*, “Phenanthro[9,10-d]imidazole as a new building block for blue light emitting materials,” *Journal of Materials Chemistry*, vol. 21, no. 14, pp. 5451–5456, 2011, doi: 10.1039/c1jm10321k.

- [28] C. Li *et al.*, “A twisted phenanthroimidazole based molecule with high triplet energy as a host material for high efficiency phosphorescent OLEDs,” *Journal of Materials Chemistry C*, vol. 6, no. 47, pp. 12888–12895, 2018, doi: 10.1039/C8TC04218G.
- [29] J. Lincy, M. George, and M. Prabha, “A Review on Various Biological Activities of 1,3,4- Thiadiazole Derivatives,” *Journal of Pharmaceutical, Chemical and Biological Sciences*, vol. 3, no. 3, pp. 329–345, 2015.
- [30] B. Šarkanj, M. Molnar, M. Čačić, and L. Gille, “4-Methyl-7-hydroxycoumarin antifungal and antioxidant activity enhancement by substitution with thiosemicarbazide and thiazolidinone moieties,” *Food Chemistry*, vol. 139, no. 1–4, pp. 488–495, 2013, doi: 10.1016/j.foodchem.2013.01.027.
- [31] D. Ruhlandt *et al.*, “Absolute quantum yield measurements of fluorescent proteins using a plasmonic nanocavity,” *Communications Biology*, vol. 3, no. 1, pp. 1–7, 2020, doi: 10.1038/s42003-020-01316-2.
- [32] “what-is-quantum-yield.” <https://www.edinst.com/blog/what-is-quantum-yield/>.
- [33] L. A. Moreno, “Absolute Quantum Yield Measurement of Powder Samples,” *Journal of Visualized Experiments*, no. 63, May 2012, doi: 10.3791/3066.
- [34] C. Würth, M. Grabolle, J. Pauli, M. Spieles, and U. Resch-Genger, “Relative and absolute determination of fluorescence quantum yields of transparent samples,” *Nature Protocols*, vol. 8, no. 8, pp. 1535–1550, 2013, doi: 10.1038/nprot.2013.087.
- [35] J. C. Zwinkels, P. C. DeRose, and J. E. Leland, *Spectral Fluorescence Measurements*, 1st ed., vol. 46. Elsevier Inc., 2014.
- [36] C. A. Royer, “Fluorescence spectroscopy.,” *Methods in molecular biology (Clifton, N.J.)*, vol. 40, pp. 65–89, 1995, doi: 10.1385/0-89603-301-5:65.
- [37] K. V. R. Murthy and H. S. Virk, “Luminescence phenomena: An introduction,” *Defect and Diffusion Forum*, vol. 347, no. June 2015, pp. 1–34, 2014, doi: 10.4028/www.scientific.net/DDF.347.1.
- [38] T. Inari, M. Yamano, A. Hirano, K. Sugawa, and J. Otsuki, “Photophysical and electrochemical properties of thienylnaphthalimide dyes with excellent photostability,” *Journal of Physical Chemistry A*, vol. 118, no. 28, pp. 5178–5188, 2014, doi: 10.1021/jp502535n.
- [39] M. K. Nayak, “Synthesis, characterization and optical properties of aryl and diaryl substituted phenanthroimidazoles,” *Journal of Photochemistry and Photobiology A: Chemistry*, vol. 241, pp. 26–37, 2012, doi: 10.1016/j.jphotochem.2012.05.018.
- [40] Q. Li and Z. Li, “The Strong Light-Emission Materials in the Aggregated State: What Happens from a Single Molecule to the Collective Group,” *Advanced Science*, vol. 4, no. 7, p. 1600484, Jul. 2017, doi: 10.1002/advs.201600484.
- [41] W. Z. Yuan *et al.*, “Changing the Behavior of Chromophores from Aggregation-Caused Quenching to Aggregation-Induced Emission: Development of Highly Efficient Light Emitters in the Solid State,” *Advanced Materials*, vol. 22, no. 19, pp. 2159–2163, Mar. 2010, doi: 10.1002/adma.200904056.
- [42] J. Guan, C. Shen, J. Peng, and J. Zheng, “What Leads to Aggregation-Induced Emission?,” *The Journal of Physical Chemistry Letters*, vol. 12, no. 17, pp. 4218–4226, May 2021, doi: 10.1021/acs.jpclett.0c03861.
- [43] Y. Hong, J. W. Y. Lam, and B. Z. Tang, “Aggregation-induced emission: phenomenon, mechanism and applications,” *Chemical Communications*, no. 29, p. 4332, 2009, doi: 10.1039/b904665h.
- [44] V. M. Granchak, T. V. Sakhno, I. V. Korotkova, Y. E. Sakhno, and S. Y. Kuchmy, “Aggregation-Induced Emission in Organic Nanoparticles: Properties and Applications: a Review,” *Theoretical and Experimental Chemistry*, vol. 54, no. 3, pp. 147–177, Jul. 2018, doi: 10.1007/s11237-018-9558-6.

- [45] Y. Yin, H. Hu, Z. Chen, H. Liu, C. Fan, and S. Pu, "Tetraphenylethene or triphenylethylene-based luminophors: Tunable aggregation-induced emission (AIE), solid-state fluorescence and mechanofluorochromic characteristics," *Dyes and Pigments*, vol. 184, p. 108828, Jan. 2021, doi: 10.1016/j.dyepig.2020.108828.
- [46] L. Viglianti *et al.*, "Aggregation-induced emission: mechanistic study of the clusteroluminescence of tetrathienylethene," *Chemical Science*, vol. 8, no. 4, pp. 2629–2639, 2017, doi: 10.1039/C6SC05192H.